International Journal of Thermophysics, Vol. 17, No. 5, 1996

Verification of Metastable Phase Diagrams by *in situ* Measurements on Undercooled Melts[1]

Th. Volkmann,[2,3] W. Löser,[4,5] and D. M. Herlach[2]

The electromagnetic levitation technique combined with pyrometric methods have been applied to verify the metastable phase diagram of Fe–Cr–Ni alloys by *in situ* observation of phase selection processes in undercooled melts. The temperatures of levitated drops prior to solidification were determined by a two-color pyrometer and the recalescence behavior of the undercooled melt was recorded from a high-speed photosensing device with a sampling rate of 1 MHz. $Fe_{69}Cr_{31-x}Ni_x$ alloy melts with different Cr/Ni ratios were investigated for undercooling levels up to 320 K. The transition from single- to double-recalescence behavior was found beyond a critical undercooling level for primary austenitic alloys with Cr/Ni < 1.5. For the first time, this gives direct evidence of metastable phase formation in this alloy system from *in situ* observations. The dendrite growth velocity displayed a sudden drop at the critical undercooling level, confirming the metastable phase formation. The intermediate arrest temperature of the double-recalescence event fits well with the calculated metastable liquidus line derived from a subregular solution model for the Gibbs free energy.

KEY WORDS: metastable phase formation; rapid solidification; stainless steel alloys; temperature measurements; undercooled melts.

1. INTRODUCTION

In many cases thermodynamic data for metastable phase formation in undercooled melts necessary for establishing metastable phase diagrams are

[1] Paper presented at the Fourth International Workshop on Subsecond Thermophysics, June 27–29, 1995, Köln, Germany.

[2] Institut für Raumsimulation, DLR Köln, P.O. Box 906058, D-51140 Köln, Germany.

[3] Present address: INTOSPACE G.m.b.H., Sophienstr. 6, D-30159 Hannover, Germany.

[4] Institut für Metallische Werkstoffe, IFW Dresden, P.O. Box 270016, D-01171 Dresden, Germany.

[5] To whom correspondence should be addressed.

0195-928X/96/0900-1217$09.50/0

not accessible to direct measurements. The metastable extensions of liquidus and solidus lines derived from thermodynamic data have been confirmed only a posteriori from investigations of as-solidified samples. Therefore, the main concern of the present paper is the experimental verification of the predicted phase diagram of the $Fe_{69}Cr_{31-x}Ni_x$ system by *in situ* observation of the temperature–time characteristics during the solidification process of metastable phases in undercooled melts for a wide range of compositions.

Containerless processing methods avoiding any contact of the liquid specimen with a solid wall are capable of establishing large undercooling levels, of the order of several 100 K, in metallic melts and direct observation of the thermal behavior during crystallization [1]. The large undercooling levels achieved allow metastable phases to appear on solidification of the sample, which may be compared with those occurring in rapid solidification processes on chill substrates [2]. Solidification processes in undercooled melts proceed extremely fast because the melt acts as a heat sink to take up the latent heat of fusion released. Typical solidification times are <1 ms and solidification velocities of more than $10\,\mathrm{m}\cdot\mathrm{s}^{-1}$ have been achieved. Therefore, the heat transfer to the environment during the recalescence period can be neglected and the recalescence plateau temperature can be associated with the liquidus temperature of the phase solidified from the undercooled melt.

For near-equilibrium solidification conditions in Fe–Cr–Ni melts there is a composition-dependent change of the solidification mode from the primary austenitic to the primary ferritic type if the Cr/Ni ratio exeeds ~ 1.5 [3, 4]. In preceding papers [5, 6] the preferred formation of the metastable δ-ferrite (bcc) phase in undercooled Fe–Cr–Ni melts of primary γ-austenitic (fcc) solidification type alloys was detected for compositions far beyond Cr/Ni <1.5 by X-ray diffraction investigations of quenched samples. For that reason the Fe–Cr–Ni system seems to be a good candidate for direct metastable phase diagram investigations by *in situ* observations.

2. EXPERIMENTAL METHODS

The Fe–Cr–Ni master alloys were arc melted from 99.999 wt% pure Fe, Cr, and Ni components under an Ar atmosphere. The sample mass for electromagnetic levitation was typically 1 g, corresponding to a sphere of 6-mm diameter. The sketch of the levitation facility is shown in Fig. 1. A more comprehensive description is given elsewhere [7]. The vacuum chamber was evacuated to 10^{-8} mbar and refilled with purified 6N He/H_2 gas. The sample was repeatedly molten in that ultrapure atmosphere and

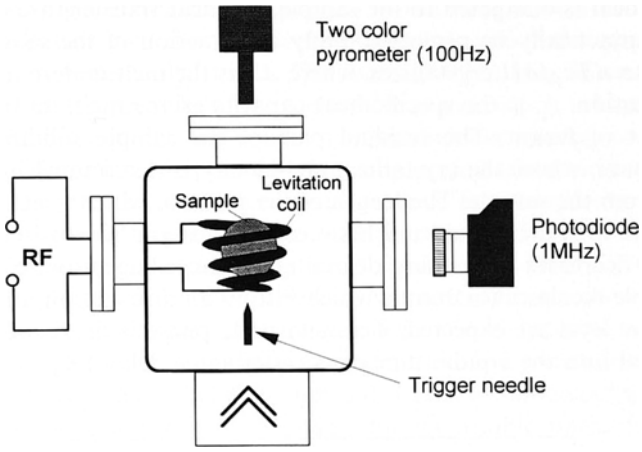

Fig. 1. Schematic diagram of the electromagnetic levitation facility for containerless undercooling experiments of liquid metals.

cooled with a He gas stream. Cooling rates of 10 to 30 $K \cdot s^{-1}$ were achieved. The temperature of the sample was monitored in absolute terms by a two-color pyrometer at a sampling rate of 100 Hz with an accuracy of <3 K.

The solidification of the melt proceeded at a preselected undercooling. To resolve details of the temperature–time characteristics during the recalescence period (<1 ms), the image of a 0.875×0.875-mm^2 section of the drop surface was projected onto a fast responding silicon photodiode with a sampling rate of 1 MHz. Measuring the time needed by the solidification front to sweep across the sample surface the dendrite growth velocity was determined with an accuracy of better than 5%.

3. RESULTS OF *IN SITU* OBSERVATIONS OF RECALESCENCE EVENTS

3.1. Time–Temperature Characteristics

The gross temperature-time charateristic during processing of an Fe–Cr–Ni sample is shown in Fig. 2. After melting, the levitated drop is overheated with respect to the liquidus temperature by an amount of 200 K and then cooled at a rate of about 10 $K \cdot s^{-1}$. When a certain degree of undercooling is achieved the fast recalescence of the particle is initiated by nucleation. During the recalescence period, which is of the order of 1 ms,

the latent heat is dissipated to the sample, but heat transfer to the environment can practically be neglected. Only one fraction of the sample corresponding to $\Delta T c_p/\Delta H$ crystallizes, where ΔT is the melt undercooling prior to solidification, c_p is the specific heat capacity of the melt, and ΔH is the latent heat of fusion. The residual part of the sample solidified in the plateau phase, where the crystallization velocity is determined by the heat removal from the sample. The length of the plateau, which is at a constant temperature for pure metals and between liquidus and solidus temperature for alloys, decreases with rising degree of undercooling prior to solidification. Double-recalescence events, which exhibit an arrest at an intermediate temperature level are expected, if a metastable phase is first nucleated and transformed into the equilibrium phase after some delay [8].

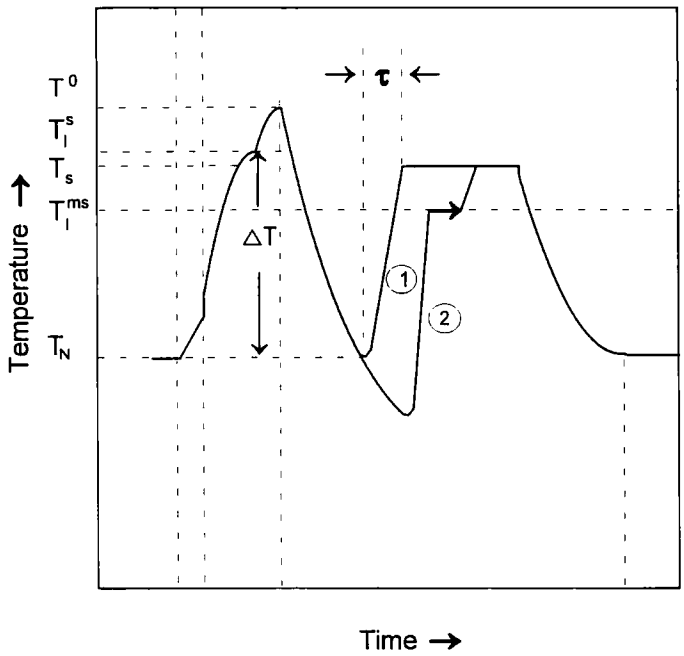

Fig. 2. Temperature–time characteristics of a levitated Fe–Cr–Ni sample. Temperature–time profiles referring to the possible solidification reaction paths: (1) crystallization of the stable phase; (2) primary crystallization of a metastable phase with subsequent transformation into the stable phase. T_N, nucleation temperature; T_l^s and T_s, liquidus and solidus temperature of the stable phase, respectively; T_l^{ms}, virtual melting temperature of the metastable phase; T_0, initial melt temperature; ΔT, undercooling; τ, recalescence time for the solidification of the stable phase.

Resolving the recalescence process of the sample by a fast-responding photodiode can give rise to direct information about the phase selection processes in undercooled melts. The thermal arrest can be ascribed to the solidification temperature of the metastable phase, which is located between the metastable liquidus and solidus temperatures in analogy to equilibrium phase solidification. Experimental examples for observation of double-recalescence events are scarce, since both a fast temperature recording facility and careful experimentation are prerequisites.

Temperature–time charateristics of recalescence events of undercooled $Fe_{69}Cr_{31-x}Ni_x$ samples with different Ni contents x are shown in Figs. 3 and 4. Clearly, in samples with compositions $x > 11$ at% Ni, which exhibit the primary austenitic solidification mode, there is a transition from single- to double-recalescence behavior beyond a critical undercooling level ΔT_c. This double-recalescence is indicative for metastable phase formation. It appears when the metastable phase is first nucleated, pushing the sample temperature to the melting temperature of the metastable phase by the latent heat released. After a short time delay, the nucleation of the equilibrium phase proceeds and the sample temperature is shifted toward the melting temperature of the equilibrium phase. The crystallization process of the residual fraction of the sample proceeds moderately by heat extraction from the drop surface. Increasing x shifts the position of the intermediate arrest to lower temperatures relative to the final plateau level, which is illustrated by comparison of Figs. 3 and 4. The length of the intermediate plateau is successively diminished with increasing x, indicating the rising thermodynamic instability of the metastable phase with increasing Ni content.

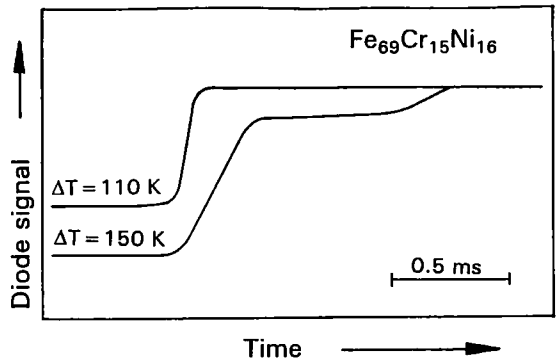

Fig. 3. Temperature–time charactaristics of recalescence events of undercooled $Fe_{69}Cr_{15}Ni_{16}$ samples with different undercooling levels ΔT prior to solidification, showing the transition from single- to double-recalescence behavior.

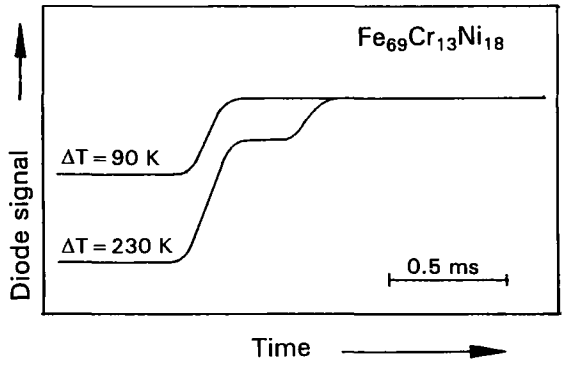

Fig. 4. Temperature–time characteristics of recalescence events of undercooled $Fe_{69}Cr_{13}Ni_{18}$ samples with different undercooling levels ΔT prior to solidification, showing, the transition from single- to double-recalescence behavior.

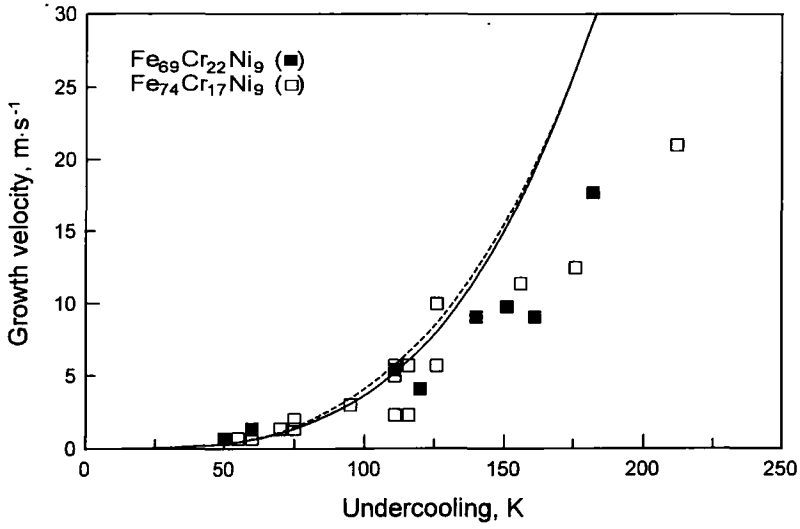

Fig. 5. Measured dendrite growth velocity in levitated undercooled $Fe_{69}Cr_{17}Ni_9$ (□) and $Fe_{69}Cr_{22}Ni_9$ (■) samples vs melt undercooling prior to solidification in comparison with calculated dendrite velocities for the growth of the equilibrium bcc phase for the respective alloy composition ($Fe_{69}Cr_{17}Ni_9$, solid line; and $Fe_{69}Cr_{22}Ni_9$, dashed line).

3.2. Dendrite Growth Kinetics

The growth kinetics of the competing phases might be considered as a possible indication for the transition from fcc to bcc primary solidification. The dendrite growth velocity as a function of the undercooling prior to solidification for the two primary ferritic solidification type alloys $Fe_{69}Cr_{22}Ni_9$ and $Fe_{74}Cr_{17}Ni_9$; shown in Fig. 5, exhibits a monotonous behavior. The experimental results may be well compared with the dendrite growth model of Lipton et al. [9], which was applied to the Fe–Cr–Ni case [10]. In the opposite case, the primary austenitic solidification type alloy $Fe_{69}Cr_{15}Ni_{16}$, the dendrite growth velocity vs ΔT characteristic presented in Fig. 6 exhibits a remarkable drop at a critical undercooling level near 150 K. From the dendrite growth theory, we derived monotonously increasing dendrite growth velocities vs ΔT for both fcc and bcc phases. The growth velocity of the metastable bcc phase is shown to be considerably smaller than that of the fcc phase. The drop in growth velocities at a critical undercooling level can be interpreted as an additional hint to the predicted transition to the metastable growth mode. On the other hand, the experimental results show that there is no kinetic advantage of the metastable bcc phase, which could give rise to a preferred growth compared with the fcc equilibrium phase.

3.3. Metastable Phase Diagram

Despite the uncalibrated temperature registration with the silicon photodiode, the location of the intermediate arrest relative to the final plateau can be used to estimate the soliditification temperature of the metastable phase. In that way, the metastable phase diagram shown in Fig. 7 was established. The experimental results are superimposed with the predicted equilibrium phase diagram and metastable extensions (dashed) of liquidus and solidus lines derived on the basis of a subregular solution model for the Gibbs free energy of Chuang and Chang [11]. There is some slope in the relation of the metastable solidification temperature with increasing Ni content. This tendency fits well to the calculated liquidus and solidus lines of the metastable bcc phase. The experimental results of *in situ* measurements reproduce reasonably well the calculated phase diagram. The bcc structure of the metastable phase was verified by X-ray diffraction analyses of as-solidified samples, which were quenched into a liquid metal pool to prevent the decay of the metastable phase to the fcc equilibrium structure.

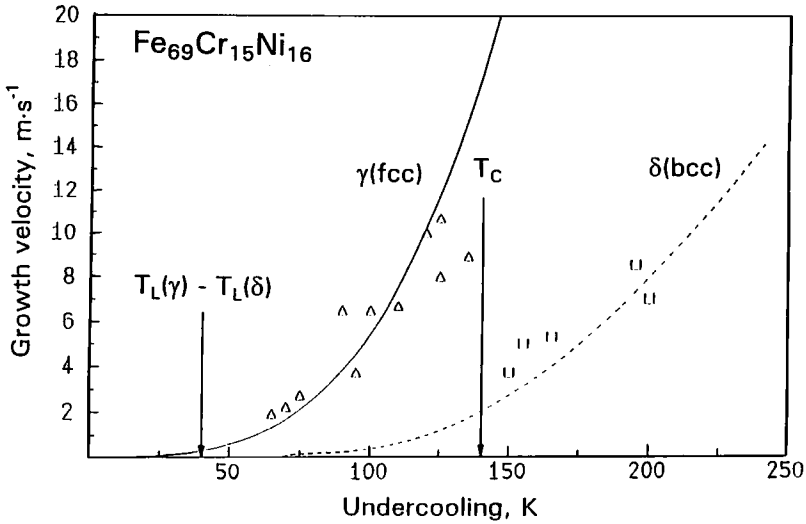

Fig. 6. Measured dendrite growth velocities in levitated undercooled $Fe_{69}Cr_{15}N_{16}$ samples vs melt undercooling prior to solidification (Δ, $\square$) in comparison with calculated velocities for the growth of the equilibrium fcc phase (solid line) and the metastable bcc phase (dashed line). The difference of the calculated liquidus temperatures $T_L(\gamma) - T_L(\delta)$ and the critical undercooling level T_c are indicated.

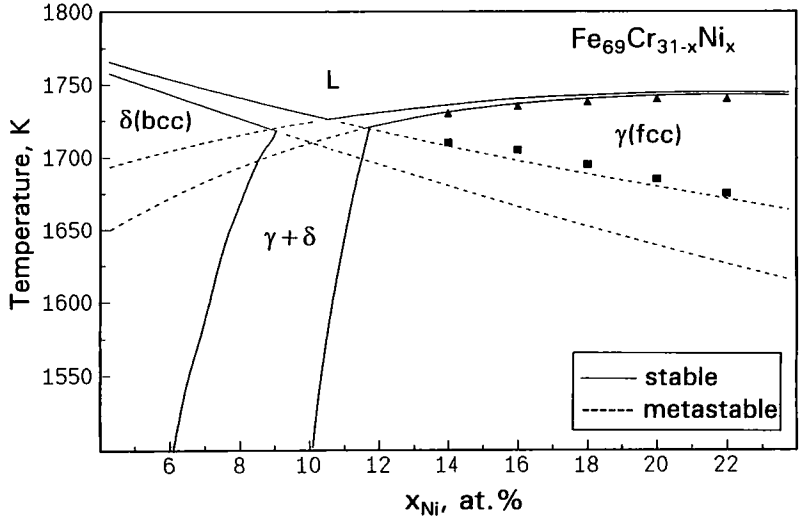

Fig. 7. Metastable phase diagram derived from the arrest positions for single-step (triangles) and two-step (squares) recalescence events. Superimposed: calculated equilibrium phase diagram (solid lines) and metastable extensions (dashed lines).

4. DISCUSSION

Subsecond measurements of the thermal history of levitated undercooled melt samples, which displayed double-recalescence events, give direct evidence of metastable phase formation in primary austenitic solidification type Fe–Cr–Ni alloys beyond Cr/Ni <1.5. The critical undercooling level ΔT_c necessary for metastable phase formation was attributed to the first occurrence of a double-recalescence event for a given alloy composition. It was found that ΔT_c increases with Ni content x. From the *in situ* measurement at maximum undercooling levels near 300 K, an ultimate $x=22$ for the metastable bcc phase formation in Fe–Cr–Ni was derived. This corresponds to Cr/Ni ≈ 0.41, which is far beyond the equilibrium phase boundary Cr/Ni ≈ 1.5. The limits derived from the direct observation may be compared with results of X-ray diffraction measurements on quenched samples where the bcc reflections were detected up to $x=16$, corresponding to Cr/Ni ≈ 0.94. This means that the subsecond measurement of the thermal history by a high-speed photosensing device is much more sensitive in detecting metastable phase formation events than the a posteriori analysis of as-solidified samples.

The intermediate arrest temperature depends on the alloy composition but is virtually independent of the undercooling level prior to solidification. It could be associated with the solidification temperature of the metastable phase. In that way, the calculated metastable phase diagram was verified experimentally. The measured dendrite growth velocity vs undercooling characteristics, which exhibit a sudden drop at a critical undercooling level, support the predicted transition from primary austenite to metastable ferrite solidification. Since the growth velocity of the metastable phase turned out to fall below that of the equilibrium phase, a superior growth kinetics of the metastable phase can be ruled out to be responsible for the observed phase selection phenomena. According to a careful theoretical investigation [6], the primary cause for the transition from fcc to metastable bcc phase formation is the competitive nucleation in the undercooled melts.

In situ observations of levitated undercooled melt drops provide a powerful tool to reveal phase selection phenomena, which have been utilized to verify metastable phase diagrams. It would be interesting to ascertain whether the metastable solidification pathways could be altered by appropriate seeding of bulk undercooled melts according to the technique used by Schleip et al. [8].

The application of the method to phase selection phenomena of undercooled melts of different alloy sytems is of future interest. Carefully projected low-gravity experiments are expected to allow still higher undercooling levels and new solidification pathways.

ACKNOWLEDGMENTS

This work was supported by Deutsche Forschungsgemeinschaft Grant He 1601/2-2 and Deutsche Agentur für Raumfahrtangelegenheiten Grant 50 WM 9232-0. The authors express their gratitude to Prof. B. Feuerbacher for continuous support of the work.

REFERENCES

1. D. M. Herlach, R. F. Cochrane, I. Egry, H. J. Fecht, and A. L. Greer, *Int. Mater. Rev.* **38**:273 (1993).
2. D. M. Herlach, *Mater. Sci. Eng.* **R12**:177 (1994).
3. N. Suutala, T. Takalo, and T. Moisio, *Metall. Trans.* **11A**:717 (1980).
4. V. G. Rivlin and G. V. Raynor, *Int. Metals Rev* **248**:21 (1980).
5. W. Löser. T. Volkmann, and D. M. Herlach, *Mater. Sci. Eng.* **A178**:163 (1994).
6. T. Volkmann, W. Löser, and D. M. Herlach, submitted for publication.
7. R. Willnecker, *Thesis* (Bochum, 1988).
8. E. Schleip, D. M. Herlach, and B. Feuerbacher, *Europhys. Lett.* **11**:751 (1990).
9. J. Lipton, W. Kurz, and R.Trivedi, *Acta Metall.* **35**:957 (1987).
10. W. Löser and D. M. Herlach, *Metall. Trans.* **23A**:1585 (1992).
11. Y. Y. Chuang and Y. A. Chang, *Metall. Trans.* **18A**:733 (1987).